A complete frequency-field diagram for the antiferromagnetic resonance in MnF_2

Masayuki Hagiwara and Koichi Katsumata
Magnetic Materials Laboratory, RIKEN

We performed antiferromagnetic resonance (AFMR) measurements on a prototypical example of antiferromagnets with uniaxial anisotropy, MnF_2 for the frequency between 20 GHz and 570 GHz and in magnetic fields up to 20 T. We have observed all the resonance branches predicted by the theory. We also measured the temperature dependence of AFMR signals and found good agreement with the theory.

In the Magnetic Materials Laboratory, we are now building an electron spin resonance (ESR) spectrometer with wide frequency and field ranges. The aim of this development is as follows: In an electron paramagnetic resonance (EPR), the resonant frequency (ν) is simply proportional to the magnetic field (H), so that we don't need a wide frequency-field window. However, in an antiferromagnetic resonance (AFMR), for example, this simple ν-H relation is not followed due to the exchange interaction and the magnetic anisotropy. In order to test our ESR spectrometer, we performed ESR measurements[1,2] on a single crystal sample of MnF_2 which is a prototypical example of antiferromagnets with uniaxial anisotropy. In the present paper, we report the results of ESR measurements on MnF_2. We were successful in observing all of the AFMR modes expected from the theory.[3,4] Moreover, we have found a significant contribution of the non-linear term in the expression of the AFMR frequency to the temperature dependence of the resonance point in the high field and low-frequency region.

The crystal structure of MnF_2 belongs to a tetragonal space group with two molecules per unit cell.[5] From the neutron scattering study by Erickson[6] below the Néel temperature ($T_N = 67.34$ K), the spins at body center sites point antiparallel to those at the corner sites with the spin easy axis parallel to the c axis. The main origin of the magnetic anisotropy is the dipole-dipole interactions.

Single crystals of MnF_2 were grown by the Bridgman method and a thin disc of MnF_2 with the c axis perpendicular to the plane was cut from a large crystal. Since many unexpected resonance lines were observed in an as-grown crystal of MnF_2, we used the single crystal which was annealed at a temperature just below the melting temperature followed by etching.[1]

In order to characterize the magnetic properties, we measured the temperature dependence of the magnetization (M) under an external field (H) using a SQUID magnetometer (Quantum Design's MPMS2). The results are shown in Fig. 1. There is no anisotropy in the susceptibility (M/H) along the c axis ($\chi_{//}$) and c plane ($\chi_\perp$) above about 67 K. On the other hand, $\chi_{//}$ and $\chi_\perp$ behave quite differently below about 67 K, which is a typical behavior below T_N in an antiferromagnet with uniaxial anisotropy.

We show in Fig. 2 an example of ESR signals obtained at 1.8 K for the frequency of 208 GHz when the external magnetic field is applied to the c axis. Figure 3 summarizes all the AFMR data obtained at 1.8 K or 5 K in the frequency-magnetic field plane.

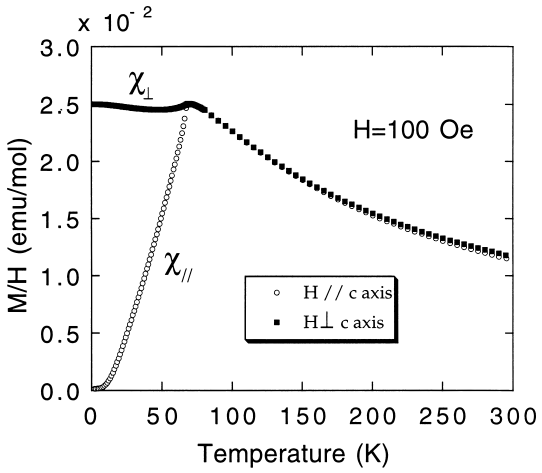

Fig. 1. The temperature dependence of the molar magnetic susceptibilities parallel and perpendicular to the c axis of MnF_2.

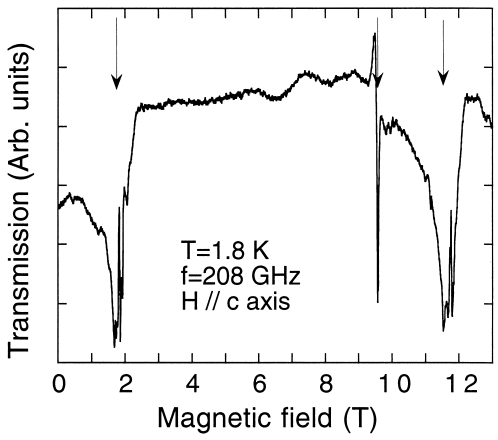

Fig. 2. Typical example of ESR signals obtained at 1.8 K for the frequency of 208 GHz when the external field applied to the c axis. Arrows show the AFMR signal positions.

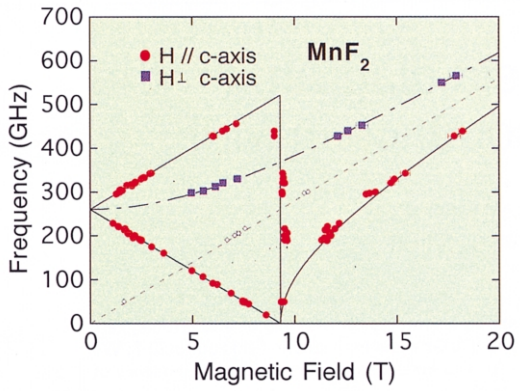

Fig. 3. Frequency versus external magnetic field relations of the AFMR signals in MnF_2. The full straight lines, the full curve and the dash-dotted line are the theoretical ones discussed in the text. The dotted line is the paramagnetic resonance line with $g = 2.0$.

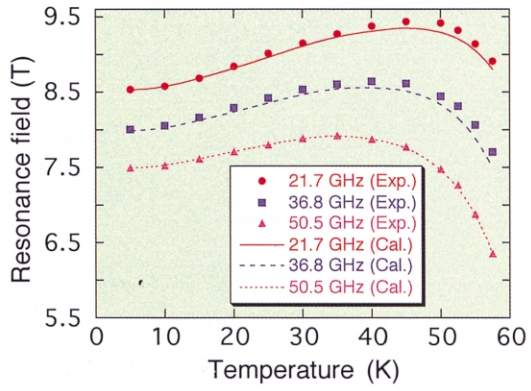

Fig. 4. The temperature dependence of the AFMR positions at the designated frequencies. The curves are the theoretical ones discussed in the text.

We have measured the temperature dependence of the resonance field in one of the AFMR modes at fixed frequencies as shown in Fig. 4. All of the resonance fields at 21.7, 36.8 and 50.5 GHz have similar behavior with increasing temperature. Namely, resonance fields increase with increasing temperature and then decrease with further increase in temperature.

In the following, we analyze the experimental results shown in Figs. 3 and 4. If the exchange field (H_e) is much larger than the anisotropy field (H_a), the AFMR frequencies of a uniaxial magnet are given by Eqs. (1)–(3) below.[7,8] In MnF_2, $H_e \sim 53\,T$ and $H_a \sim 0.82\,T$ so that $H_e \gg H_a$.[9]

$$h\nu/g\mu_B = \sqrt{2K_u/\chi_\perp + (\chi_{//}H/2\chi_\perp)^2} \pm H(1 - \chi_{//}/2\chi_\perp) \quad (H//c,\ H < H_{SF}), \qquad (1)$$

$$h\nu/g\mu_B = \sqrt{H^2 - 2K_u/\chi_\perp} \quad (H//c,\ H > H_{SF}), \qquad (2)$$

and

$$h\nu/g\mu_B = \sqrt{H^2 + 2K_u/\chi_\perp} \quad (H \perp c), \qquad (3)$$

where h is Plank's constant, g the g-value, μ_B the Bohr magneton, K_u the anisotropy constant and H_{SF} the critical field for spin flop. At low temperatures ($T \ll T_N$), $\chi_{//}$ is much smaller than $\chi_\perp$, so Eq. (1) becomes

$$h\nu/g\mu_B = \sqrt{2K_u/\chi_\perp} \pm H. \qquad (4)$$

The two full straight lines below 9.3 T in Fig. 3 represents Eq. (4), the full curve above 9.3 T Eq. (2) and the broken curve Eq. (3) with $\sqrt{2K_u/\chi_\perp} = 9.27\,T$. This value of the zero field gap frequency (259.7 GHz) is very close to that reported before (261.4 ± 1.5 GHz at 0 K).[9] The vertical straight line at 9.27 T represents the critical field resonance mode. We see in Fig. 3 good agreement between theory and experiment. In the present study, we complete the frequency-field chart for all the AFMR modes in MnF_2.

Next, we analyze the temperature dependence of the resonance field (Fig. 4). The frequency-field relation of the AFMR mode relevant to the data in Fig. 3 is given by Eq. (1) with the minus sign. In this equation, K_u, $\chi_{//}$ and $\chi_\perp$ depend on temperature. We use for the temperature dependence of the ratio of $\chi_{//}/\chi_\perp$ the experimental values shown in Fig. 1. The g-value is obtained from Fig. 3 to be 2.00. Then, we have only one adjustable parameter, $K_u/\chi_\perp$. We obtain the temperature dependence of $K_u/\chi_\perp$ by fitting Eq. (1) with the data taken at 50.5 GHz. We can then compare the theory with the experiments performed at 21.7 and 36.8 GHz without any adjustable parameters. The agreement between the theory and the experiment at both frequencies is satisfactory. The broad peak in the temperature dependence of the resonance fields originates from the combined effect of the two terms, $2K_u/\chi_\perp$ and $(\chi_{//}H/2\chi_\perp)^2$ in Eq. (1).

In summary, we have made ESR measurements on a well characterized single crystal of MnF_2 using a wide-frequency and high-field spectrometer installed in RIKEN. We have been successful in observing all the AFMR modes expected for an antiferromagnet with uniaxial anisotropy. We have also observed the effect of the non-linear term on the temperature dependence of the AFMR position. All these experimental results agree quantitatively with the theory.

This work was done in collaboration with P. Goy, M. Gross, H. Suzuki, M. Tokunaga, I. Yamada, and H. Yamaguchi.

References

1) M. Hagiwara, K. Katsumata, I. Yamada, and H. Suzuki: J. Phys.: Condens. Matter. **8**, 7349 (1996).
2) M. Hagiwara, K. Katsumata, H. Yamaguchi, M. Tokunaga, I. Yamada, M. Gross, and P. Goy: Int. J. Infrared Millimeter Wave **20**, 617 (1999).
3) T. Nagamiya: Prog. Theor. Phys. **6**, 342 (1951).
4) F. Keffer and C. Kittel: Phys. Rev. **85**, 329 (1952).
5) M. Griffel and J. W. Stout: J. Am. Chem. Soc. **72**, 4351 (1950).
6) R. A. Erickson: Phys. Rev. **90**, 779 (1953).
7) T. Nagamiya, K. Yosida, and R. Kubo: Adv. Phys. **4**, 1 (1955).
8) S. Foner: Phys. Rev. **107**, 683 (1957); in *Magnetism* Vol. 1, edited by G. T. Rado and H. Suhl, (Academic Press, New York, 1963), p. 383.
9) F. M. Johnson and A. H. Nethercot, Jr.: Phys. Rev. **114**, 705 (1959).